ANIMAL CELLS AND SYSTEMS
2024, VOL. 28, NO. 1, 536–550
https://doi.org/10.1080/19768354.2024.2417458

Taylor & Francis
Taylor & Francis Group

AP001885.4 promotes the proliferation of esophageal squamous cell carcinoma cells by histone lactylation- and NF-κB (p65)-dependent transcription activation and METTL3-mediated mRNA stability of c-myc

Chuang Fu[a]*, Wen Jiang[b]*, Chong Wang[a], Sheng-Jie Song[a], Hao Tao[a], Xin-Guo Zhang[a], Wen-Ting Li[a], Xin Jin[a], Bin-Bing Yu[c], Jia-Jie Hao[d], Wen-Juan Sun[e], Jie Bai[a] and Zhi-Zhou Shi[a]

[a]Medical School, Kunming University of Science and Technology, Kunming, People's Republic of China; [b]Department of Thoracic Surgery, the Affiliated Hospital of Kunming University of Science and Technology and First People's Hospital of Yunnan Province, Kunming, People's Republic of China; [c]Department of Anus & Intestine Surgery, Kunming Municipal Hospital of Traditional Chinese Medicine, Kunming, People's Republic of China; [d]State Key Laboratory of Molecular Oncology, Center for Cancer Precision Medicine, National Clinical Research Center for Cancer/Cancer Hospital, National Cancer Center, Chinese Academy of Medical Sciences (CAMS), Peking Union Medical College (PUMC), Beijing, People's Republic of China; [e]Nephrology Division, Pu'er People's Hospital, Pu'er, People's Republic of China

ABSTRACT

Esophageal squamous cell carcinoma (ESCC) is an aggressive malignant neoplasm, and up to now, the role of long non-coding RNA (lncRNA) AP001885.4 in cancer, including ESCC, is absolutely unclear. The GEPIA database was applied to identify differentially expressed and prognosis-associated genes in esophageal cancer (ESCA). CCK-8, colony formation, Western blot, and qRT-PCR methods were harnessed to investigate the role and mechanism of AP001885.4 in esophageal carcinogenesis. By analyzing TCGA data in the GEPIA database, two lncRNAs were selected. AP001885.4 was overexpressed and positively associated with the unfavorable outcome of ESCC patients, and LINC001786 was under-expressed and negatively linked with the poor prognosis. Knockdown of AP001885.4 suppressed the proliferation and colony formation of ESCC cells. Importantly, the silence of AP001885.4 downregulated c-myc. Mechanically, the knockdown of AP001885.4 reduced METTL3 expression and m6A modification in c-myc mRNA, and METTL3 positively regulated c-myc. Furthermore, the knockdown of AP001885.4 diminished histone lactylation and NF-κB (p65) expression, and the protein lactylation inhibitors (2-DG, 2-deoxy-D-glucose and oxamate) and the NF-κB inhibitor (JSH-23) also lessened c-myc expression. Consequently, our findings suggested that AP001885.4 promoted the proliferation of esophageal squamous cell carcinoma cells by histone lactylation- and NF-κB (p65)-dependent transcription activation and METTL3-mediated mRNA stability of c-myc.

ARTICLE HISTORY
Received 25 June 2024
Revised 2 September 2024
Accepted 6 October 2024

KEYWORDS
AP001885.4; C-myc; lactylation; NF-κB; ESCC

1. Introduction

Esophageal cancer is the sixth most common tumor and the fifth most common tumor death in China (Zheng et al. 2023). Squamous cell carcinoma (SCC) and adenocarcinoma (AD) are two major subtypes of esophageal cancer, and ESCC accounts for about ninety percent of all esophageal cancer cases (Arnold et al. 2015). Therefore, elucidating the carcinogenic mechanisms and identifying therapeutic targets in ESCC are imminent.

Esophageal tumorigenesis is a complicated process. Previous studies have reported that dysregulated PD-1 (Smyth et al. 2021), p53(Ohashi et al. 2015), and lncRNA SNHG16 (Ren et al. 2022) participated in the carcinogenesis of the esophagus. LncRNA is one type of non-coding RNA with lengths of more than 200 nucleotides and plays critical roles in carcinogenesis (Chen, Wang, et al. 2022; Nair et al. 2020; Roh et al. 2023). A lot of lncRNAs played crucial roles in ESCC. LncRNA ESCCAL-1 directly bound and suppressed ubiquitin-mediated degradation of galectin-1, and finally promoted the cell proliferation of ESCC cells (Cui et al. 2022). LncRNA DLEU1 bound and suppressed ubiquitination and proteasomal degradation of DYNLL1, and eventually upregulated BCL2 and inhibited apoptosis of ESCC cells (Li et al. 2022). LncRNA TMPO-AS1 promoted ESCC cell proliferation and metastasis by transcriptionally

CONTACT Zhi-Zhou Shi zhizhoushi@kust.edu.cn Medical School, Kunming University of Science and Technology, No.727, Jingming South Road, Kunming 650500, People's Republic of China
*Contributed equally.

Supplemental data for this article can be accessed online at https://doi.org/10.1080/19768354.2024.2417458.

activating TMPO through recruiting p300 to the promoter of *TMPO* gene (Luo et al. 2022). LncRNA JPX improved the invasion, migration, and proliferation of ESCC cells through affecting the VEGFA/miR-516b-5p axis (Hu et al. 2016).

Through analyzing the TCGA data (GEPIA database), AP001885.4 was selected as a unique overexpressed and poor prognosis-associated lncRNA in ESCA. AP001885.4 is located in the intron of the *KDM2A* gene (11q13.2). 11q13 is highly amplified in ESCC and head and neck squamous cell carcinoma (HNSCC) (Cancer Genome Atlas 2015; Shi et al. 2011, 2013). Nevertheless, the role of AP001885.4 in cancer is absolutely unknown.

Our data in this study indicated that the knockdown of AP001885.4 repressed the colony formation and proliferation of ESCC cells and downregulated c-myc. Then, we further investigated the mechanism of how AP001885.4 regulated c-myc in ESCC.

2. Materials and methods

2.1. Tissue samples

Nine paired tissue samples from patients of ESCC were collected by the Thoracic Surgery Department at the Affiliated Hospital of Kunming University of Science and Technology and First Hospital of Yunnan Province (Kunming, China). Every patient signed an informed consent form without any treatment before surgery. The Medical Ethics Committee of Kunming University of Science and Technology approved this study.

2.2. Cell culture

EC109, KYSE510, KYSE450, KYSE410, KYSE150, KYSE140, KYSE70, and KYSE30 cells were cultured using 10% FBS (Gibco, USA) containing RPMI-1640 medium (100 μg/mL streptomycin and 100 U/mL penicillin) at 5% CO_2 and 37°C.

Lipofectamine 2000 (Thermo, USA) was harnessed to transfect siRNAs (GenePharma, China) into cells following the manufacturer's instructions. Sequences of siRNAs are listed: AP001885.4 si1 sense, 5′-GCCAUCUGGCUGACAUGAATT-3′, antisense, 5′-UUCAUGUCAGCCAGAUGGCTT-3′; AP001885.4 si2 sense, 5′-GCCCUAAUAUGGGUGACUATT-3′, antisense, 5′-UAGUCACCCAUAUUAGGGCTT-3′; LDHA siRNA sense, 5′-AGACCCUUAAUCAUGGUGGTT-3′, antisense, 5′-CCACCAUGAUUAAGGGUCUTT-3′; LDHB siRNA sense, 5′-GGUGUCUGAAGAAAUAAGCTT-3′, antisense, 5′-GCUUAUUUCUUCAGACACCTT-3′; negative control siRNA sense, 5′-UUCUCCGAACGUGUCACGUTT-3′, antisense, 5′-ACGUGACACGUUCGGAGAATT-3′.

2-DG, oxamate, and JSH-23 were obtained from Selleck Chemicals (USA).

2.3. qRT-PCR assay

HifiScript cDNA Synthesis Kit (Cwbiotech, Beijing, China) and PowerUp™ SYBR™ Green Master Mix (Thermo, USA) were used in the qRT-PCR assay. Sequences of primers (Tsingke, China) are listed. AP001885.4-1, forward primer, 5′-GGCAACGGAACCAGCTTTGA-3′, and reverse primer, 5′-GCCAACAATTGTCAGCTTGTCC-3′; AP001885.4-2, forward primer, 5′-GTAATAGGCCCACTTGCTCCC-3′, and reverse primer, 5′-GATGCAGGCTACCACTGCTG-3′; LINC01785, forward primer, 5′-ATCCAGCCTGCCTCCATTAC-3′, and reverse primer, 5′-AAAACAGTTTGGCCTGCCCT-3′; CCND1, forward primer, 5′-TGGTGAACAAGCTCAAGTGGA-3′, and reverse primer, 5′-AGGGCGGATTGGAAATGAACT-3′; CCNE1, forward primer, 5′-TGACCTAAGGGACTCCCACAA-3′, and reverse primer, 5′-TGATAATGTGGAGAGGGCAGC-3′; c-MYC, forward primer, 5′-GTCAAGAGGCGAACACACAAC-3′, and reverse primer, 5′-TTGGACGGACAGGATGTATGC-3′; METTL3, forward primer, 5′-CCCTATGGGACCCTGACAGA-3′, and reverse primer, 5′-CTGGTTGAAGCCTTGGGGAT-3′; RELA, forward primer, 5′-CTGGCATCCGTCGACAACTCC-3′, and reverse primer, 5′-TCACTAGGCGAGTTATAGCCTC-3′; LDHA, forward primer, 5′-GACGTGCATTCCCGATTCCT-3′, and reverse primer, 5′-AAGGCTGCCATGTTGGAGAT-3′; GAPDH, forward primer, 5′-AAATCCCATCACCATCTTC-CAG-3′, and reverse primer, 5′-GAGTCCTTCCACGATAC-CAAAGTTG-3′.

2.4. Cell proliferation and colony formation assays

Cell proliferation and colony formation abilities are measured using CCK-8 (Cell Counting Kit-8, Dojindo Laboratories, Japan) and colony formation assays following previously described (Mei et al. 2017).

2.5. Western blot assay

Western blot procedure is referred to our previous description (Shi et al. 2020). The antibodies' information is METTL3 antibody (15073-1-AP), p65 antibody (66535-1-Ig), GAPDH antibody (60004-1-Ig), ALKBH5 antibody (16837-AP), ELAVL1 antibody (11910-1-AP) and Histone-H3 antibody (17168-1-AP) from Proteintech, c-MYC antibody (18583) from Cell Signaling Technology, and L-Lactyl Lysine antibody (PTM-1401RM) and L-Lactyl-Histone H3 (Lys18) antibody (PTM-1406RM) from PTMBIO.

2.6. Chromatin immunoprecipitation assay (ChIP)-qPCR

The objective of this study is to investigate the interaction between H3K18la and the promoter regions of c-MYC and AP001885.4, as well as the interaction

between P65 and the promoter region of c-MYC. To achieve this, we utilized a SimpleCHIP® Plus Enzymatic Chromation IP Kit (Magnetic Beads) (CST 9003, USA) following the manufacturer's protocol. Sequences of primers (Tsingke, China) are listed, chip-(c-myc)-a, forward primer, 5′-GTGCAGTGCATCGGATTTGG-3′, and reverse primer, 5′-GGGGTGCGTGTATAGCATGT-3′; chip-(c-myc)-b, forward primer, 5′-CTTTGGGTGAGGGAC-CAAGG-3′, and reverse primer, 5′- CCCCACACAT-GATTTGTTT-3′; chip-(c-myc)-c, forward primer, 5′-GGCTTGGCGGGAAAAAGAAC-3′, and reverse primer, 5′-CTCGCTGGAATTACTACAGCG-3′; chip-(c-myc)-d, forward primer, 5′-TGCAGCTATCATTTGCAACACC-3′, and reverse primer, 5′- GAGGCTTTGGACACACCCAA-3′; chip-AP001885.4, forward primer, 5′-ATTCCTTATTGGAGCC-TATTGAGA-3′, and reverse primer, 5′- ACCCAGTT-CAAAGCTGGTTC-3′.

2.7. RIP-PCR

The m6A-modification of c-MYC and RELA mRNA, and the interaction between AP001885.4 and LDHA/LDHB were detected using the RIP assay. Briefly, 1.0×10^7 cells were treated with 400 µL of RIP lysis buffer. From this, 40 µL of supernatant was used as input, while 160 µL of supernatant was incubated overnight at 4°C with m6A antibody or rabbit IgG-coupled protein A/G magnetic beads in IP buffer supplemented with an RNase inhibitor. After washing, the immunoprecipitated RNA was digested, purified, and subsequently subjected to qPCR analysis. Sequences of primers (Tsingke, China) are listed. AP001885.4-2, forward primer, 5′-GTAA-TAGGCCCACTTGCTCCC-3′, and reverse primer, 5′-GATG-CAGGCTACCACTGCTG-3′; c-MYC, forward primer, 5′-GTCAAGAGGCGAACACACAAC-3′, and reverse primer, 5′-TTGGACGGACAGGATGTATGC-3′; RELA, forward primer, 5′-CTGGCATCCGTCGACAACTCC-3′, and reverse primer, 5′-TCACTAGGCGAGTTATAGCCTC-3′.

2.8. Bioinformatic analysis and structure predictions

The GSE35622 and GSE35624 datasets were acquired from the Gene Expression Omnibus (GEO) database. The catRAPID database (Bellucci et al. 2011) was utilized to identify proteins capable of interacting with the specified lncRNAs. Initial analysis of the predicted structure was obtained from the AlphaFold3 Protein Structure Database (https://alphafoldserver.com/).

2.9. Intracellular lactate concentration

Intracellular lactate concentrations were quantified using a lactate assay kit (Solarbio, Beijing, China, BC2235) in accordance with the manufacturer's guidelines. In summary, cellular samples were homogenized in Lactate Assay Buffer and mixed with a Master Reaction Mix containing Lactate Probes. The absorbance values were measured at 570 nm using a spectrophotometer. The lactate content was normalized based on the cell number.

2.10. Statistical analysis

GraphPad Prism 9 software (La Jolla, CA, USA) is harnessed to analyze the data. Quantitative data are shown as the mean ± SD and are analyzed by ANOVA or student's t-test. $P < 0.05$ is defined as a statistical significance.

3. Results

3.1. AP001885.4 is elevated and positively correlated with poor prognosis in esophageal cancer

Based on the GEPIA database, we identified 58 genes that meet the conditions of overexpressed together with poor prognosis-associated and under-expressed together with good prognosis-associated in ESCA (Table 1, Table S1, and Table S2). Among them, two lncRNAs, including AP001885.4 (also known as RP11-157K17.5 and ENSG00000179038.8) and LINC01786 (also known as RP5-902P8.10 and ENSG00000230415.1), were selected (Figure 1A). In ESCA, AP001885.4 was overexpressed, and its high expression was significantly correlated with unfavorable outcomes of patients (Figure 1B and C), whereas LINC01786 was lowly expressed, and its low expression was remarkably linked with patients' unfavorable outcomes (Figure S1A and S1B). Pan-cancer analysis of TCGA data showed that AP001885.4 expression was increased in many forms of cancers, such as ESCA and stomach cancer (STAD), and LINC001786 was under-expressed in many types of cancers, such as ESCA and colon cancer (COAD) (Figure 1D and S1C). After analyzing the TCGA Copy Number portal database, we found that *KDM2A*, the host gene of AP001885.4, was amplified in 17.26% of all cancers and 19.06% of epithelial cancers (Figure 1E), indicating amplification is a reason for its overexpression in cancers. qRT-PCR assay confirmed that AP001885.4 was overexpressed in 5 of 9 ESCC cases, whereas LINC01786 exhibited inconsistent changes in ESCC cases (Figure 1F and S1D). Accordingly, we select AP001885.4 for further study.

3.2. Knockdown of AP001885.4 suppresses the colony formation and proliferation of ESCC cells

AP001885.4 has two transcripts, including ENST00000621658 and ENST00000444002, and is

Table 1. Differentially expressed and survival-associated genes in esophageal cancer by analyzing GEPIA database.

NO.	Gene Symbol[1]	Official symbol[2]	Gene ID[3]	Median (Tumor)	Median (Normal)	Regulation	Log2(Fold Change)	adjp	Survival OS	*P*-Value (Survival OS)
Overexpressed and poor prognosis associated genes										
1	IDO1	IDO1	ENSG00000131203.12	7.4	0.54	Up	2.447	2.46E-36	Poor prognosis	1.46E-02
2	GNL3L	GNL3L	ENSG00000130119.15	19.965	3.56	Up	2.201	3.77E-105	Poor prognosis	2.77E-03
3	FAM46A	TENT5A	ENSG00000112773.15	11.539	2.17	Up	1.984	6.44E-44	Poor prognosis	1.10E-02
4	C2	C2	ENSG00000166278.14	18.545	3.945	Up	1.983	3.05E-35	Poor prognosis	1.23E-02
5	LRRC58	LRRC58	ENSG00000163428.3	20.669	4.585	Up	1.956	1.10E-90	Poor prognosis	2.30E-02
6	ESM1	ESM1	ENSG00000164283.12	2.99	0.1	Up	1.859	5.60E-69	Poor prognosis	1.81E-02
7	STAG2	STAG2	ENSG00000101972.18	44.719	13.485	Up	1.658	2.30E-83	Poor prognosis	2.01E-02
8	KIAA0040	KIAA0040	ENSG00000235750.9	16.515	5.17	Up	1.505	1.13E-44	Poor prognosis	2.14E-02
9	PLCD3	PLCD3	ENSG00000161714.11	73.145	25.155	Up	1.503	1.13E-28	Poor prognosis	1.22E-02
10	LRP6	LRP6	ENSG00000070018.8	10.245	3.095	Up	1.457	2.02E-48	Poor prognosis	1.80E-02
11	ANGPT2	ANGPT2	ENSG00000091879.13	4.735	1.095	Up	1.453	5.75E-44	Poor prognosis	2.65E-02
12	APLN	APLN	ENSG00000171388.11	2.29	0.21	Up	1.443	6.60E-47	Poor prognosis	1.44E-02
13	ATF3	ATF3	ENSG00000162772.16	25.842	8.88	Up	1.442	2.31E-10	Poor prognosis	8.98E-03
14	ARL5B	ARL5B	ENSG00000165997.4	15.234	4.995	Up	1.437	8.31E-55	Poor prognosis	7.24E-03
15	GLI2	GLI2	ENSG00000074047.20	3.215	0.61	Up	1.388	2.91E-36	Poor prognosis	9.47E-03
16	U1	RNU1-1	ENSG00000274210.1	1.605	0	Up	1.381	2.32E-20	Poor prognosis	5.84E-03
17	SMS	SMS	ENSG00000102172.15	64.504	24.434	Up	1.365	1.05E-53	Poor prognosis	2.58E-02
18	U1	RNU1-1	ENSG00000206828.1	1.57	0	Up	1.362	9.33E-12	Poor prognosis	5.69E-03
19	**RP11-157K17.5/ AP001885.4**	**N/A**	**ENSG00000179038.8**	**1.88**	**0.17**	**Up**	**1.3**	**2.66E-63**	**Poor prognosis**	**1.57E-02**
20	RGS16	RGS16	ENSG00000143333.6	5.62	1.715	Up	1.286	3.09E-19	Poor prognosis	1.34E-02
21	TAF3	TAF3	ENSG00000165632.7	6.655	2.235	Up	1.243	1.83E-72	Poor prognosis	2.06E-02
22	HELB	HELB	ENSG00000127311.9	2.675	0.58	Up	1.218	6.03E-54	Poor prognosis	6.75E-03
23	FAM3C2	FAM3C2P	ENSG00000174028.6	14.645	5.795	Up	1.203	4.41E-34	Poor prognosis	2.25E-02
24	MS4A7	MS4A7	ENSG00000166927.12	7.035	2.52	Up	1.191	5.24E-12	Poor prognosis	1.27E-02
25	HMGB3	HMGB3	ENSG00000029993.14	44.094	18.78	Up	1.189	1.09E-43	Poor prognosis	2.09E-02
26	GOLT1B	GOLT1B	ENSG00000111711.9	28.834	12.225	Up	1.174	3.65E-51	Poor prognosis	2.05E-02
27	ERAP2	ERAP2	ENSG00000164308.16	11.62	4.605	Up	1.171	2.97E-11	Poor prognosis	2.67E-02
28	SIRPA	SIRPA	ENSG00000198053.11	22.942	9.67	Up	1.166	1.47E-16	Poor prognosis	7.24E-03
29	MME	MME	ENSG00000196549.10	2.41	0.525	Up	1.161	2.44E-26	Poor prognosis	1.32E-02
30	TOP1	TOP1	ENSG00000198900.5	64.616	28.61	Up	1.148	3.22E-44	Poor prognosis	1.25E-02
31	ETV1	ETV1	ENSG00000006468.13	3.72	1.155	Up	1.131	7.82E-26	Poor prognosis	1.54E-02
32	SPATS2	SPATS2	ENSG00000123352.17	14.92	6.31	Up	1.123	1.49E-52	Poor prognosis	1.30E-02
33	FABP6	FABP6	ENSG00000170231.15	3.07	0.905	Up	1.095	3.67E-19	Poor prognosis	2.51E-02
34	DLEU2	DLEU2	ENSG00000231607.8	6.38	2.475	Up	1.087	1.06E-43	Poor prognosis	2.12E-02
35	KIAA1919	MFSD4B	ENSG00000173214.5	2.965	0.88	Up	1.077	1.85E-76	Poor prognosis	5.92E-04

(*Continued*)

Table 1. Continued.

NO.	Gene Symbol[1]	Official symbol[2]	Gene ID[3]	Median (Tumor)	Median (Normal)	Regulation	Log2(Fold Change)	adjp	Survival OS	*P*-Value (Survival OS)
36	AATF	AATF	ENSG00000275700.4	43.696	20.315	Up	1.068	1.17E-59	Poor prognosis	2.64E-02
37	RN7SL364P	RN7SL364P	ENSG00000243560.3	1.085	0	Up	1.06	3.41E-25	Poor prognosis	4.40E-03
38	LCP2	LCP2	ENSG00000043462.11	10.78	4.85	Up	1.01	7.18E-16	Poor prognosis	2.05E-02
39	TFAP4	TFAP4	ENSG00000090447.11	14.645	6.775	Up	1.009	2.06E-41	Poor prognosis	2.29E-02
Under-expressed and good prognosis associated genes										
1	PHYHIP	PHYHIP	ENSG00000168490.13	0.795	6.45	Down	−2.053	6.34E-68	Good prognosis	9.31E-03
2	FAM189A2	FAM189A2	ENSG00000135063.17	1.35	8.665	Down	−2.04	1.31E-65	Good prognosis	1.94E-03
3	ST3GAL4	ST3GAL4	ENSG00000110080.18	14.64	54.615	Down	−1.83	2.76E-20	Good prognosis	1.64E-02
4	PPT2-EGFL8	PPT2-EGFL8	ENSG00000258388.7	1.51	7.63	Down	−1.782	1.95E-76	Good prognosis	2.19E-02
5	NKX6-1	NKX6-1	ENSG00000163623.9	1.205	6.195	Down	−1.706	3.66E-21	Good prognosis	4.35E-03
6	MINOS1-NBL1	MICOS10-NBL1	ENSG00000270136.5	0.05	2.36	Down	−1.678	1.48E-54	Good prognosis	7.23E-03
7	ZBTB7C	ZBTB7C	ENSG00000184828.9	8.375	28.435	Down	−1.651	5.69E-17	Good prognosis	6.51E-03
8	DLK2	DLK2	ENSG00000171462.14	2.265	8.945	Down	−1.607	1.05E-10	Good prognosis	5.30E-03
9	TBX6	TBX6	ENSG00000149922.10	2.35	8.88	Down	−1.56	3.81E-27	Good prognosis	1.35E-02
10	ULK3	ULK3	ENSG00000140474.12	25.23	70.641	Down	−1.45	3.66E-38	Good prognosis	1.44E-02
11	WNT5B	WNT5B	ENSG00000111186.12	4.215	13.195	Down	−1.445	2.56E-23	Good prognosis	2.10E-02
12	OVOL1	OVOL1	ENSG00000172818.9	11.995	33.811	Down	−1.422	1.94E-12	Good prognosis	3.22E-03
13	RGL2	RGL2	ENSG00000237441.9	34.484	78.221	Down	−1.159	1.21E-31	Good prognosis	2.50E-02
14	**RP5-902P8.10**	**LINC01786**	**ENSG00000230415.1**	**0.22**	**1.675**	**Down**	**−1.133**	**2.22E-46**	**Good prognosis**	**2.34E-02**
15	PCF11	PCF11	ENSG00000165494.10	16.964	38.341	Down	−1.131	2.33E-36	Good prognosis	1.66E-02
16	SPSB3	SPSB3	ENSG00000162032.15	25.615	55.035	Down	−1.074	4.22E-31	Good prognosis	7.70E-03
17	ZFYVE21	ZFYVE21	ENSG00000100711.13	29.39	62.714	Down	−1.068	1.02E-32	Good prognosis	8.85E-03
18	THBS3	THBS3	ENSG00000169231.13	11.45	25.094	Down	−1.068	8.90E-25	Good prognosis	1.11E-02
19	UBE2Q2P2	UBE2Q2P2	ENSG00000259429.5	5.415	12.225	Down	−1.044	1.20E-14	Good prognosis	1.76E-02

Note: 1: Gene symbol in GEPIA database; 2: Official symbol in NCBI database; 3: Gene ID in Ensembl data.

located in the intron of the *KDM2A* gene (chr11q13.2), which is highly amplified in ESCC (Shi et al. 2011, 2013) (Figure 2A). By analyzing the lncLocator and CPC2.0 (Coding Potential Calculator 2) databases, these two transcripts are predicted to be dominantly expressed in the cytoplasm and have a low coding potential (Figure 2B and C). In ESCC cell lines (EC109, KYSE450, and KYSE150), the level of ENST00000444002 was higher than that of ENST00000621658 (Figure 2D). Therefore, we selected ENST00000444002 (named with AP001885.4 in the following results) and further investigated its role in ESCC.

We knocked down AP001885.4 in KYSE450 and KYSE150 cells, in which the AP001885.4 level was higher than other cell lines (Figure 2E and F). Downregulation of AP001885.4 suppressed the colony formation and proliferation of KYSE450 and KYSE150 cells (Figure 2G–I). In ESCC cells, the silence of AP001885.4 also downregulated cell cycle-associated molecules CCNE1 and CCND1 (Figure 2J and K). However, the silence of AP001885.4 couldn't affect the colony formation of KYSE70 cells in which AP001885.4 was lowly expressed (Figure S2A and S2B).

3.3. Knockdown of AP001885.4 downregulates c-myc in a METTL3-dependent way

c-myc is a well-investigated oncogene and regulates tumor cell migration, invasion, proliferation, and angiogenesis in cancers, including ESCC (Chen, Duan, et al. 2022; Lee et al. 2019; Meskyte et al. 2020). Notably, we

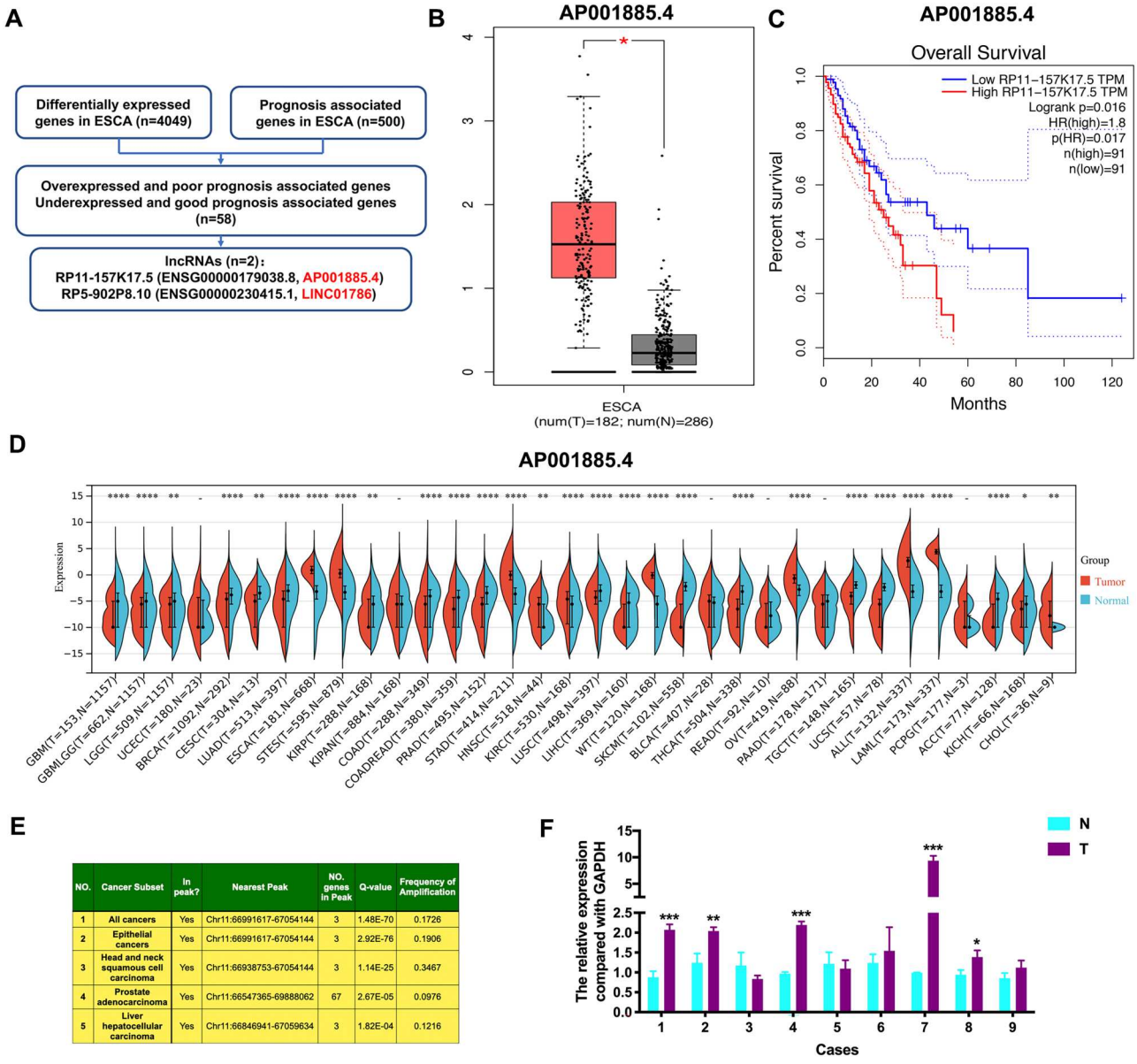

NO.	Cancer Subset	In peak?	Nearest Peak	NO. genes in Peak	Q-value	Frequency of Amplification
1	All cancers	Yes	Chr11:66991617-67054144	3	1.48E-70	0.1726
2	Epithelial cancers	Yes	Chr11:66991617-67054144	3	2.92E-76	0.1906
3	Head and neck squamous cell carcinoma	Yes	Chr11:66938753-67054144	3	1.14E-25	0.3467
4	Prostate adenocarcinoma	Yes	Chr11:66547365-69888062	67	2.67E-05	0.0976
5	Liver hepatocellular carcinoma	Yes	Chr11:66846941-67059634	3	1.82E-04	0.1216

Figure 1. AP001885.4 is elevated and positively correlated with poor prognosis in esophageal cancer. (A) Method of identifying differentially-expressed and prognosis-associated lncRNAs in ESCA. (B-C) The expression level and prognostic value of AP001885.4 (also known as RP11-157K17.5 and ENSG00000179038.8) in ESCA. (D) Pan-cancer expression of AP001885.4. (E) Amplification of the *KDM2A* gene in cancers was analyzed using the TCGA Copy Number portal database. (F) The expression level of AP001885.4 in ESCC tissues (T) and adjacent normal tissues (N). *, $p < 0.05$; **, $p < 0.01$; ***, $p < 0.001$; ****, $p < 0.0001$.

found that the silence of AP001885.4 remarkably downregulated c-myc in mRNA and protein levels (Figure 3A–C). m6A methylation modification participates in the regulation of mRNA stability. Hence, we further evaluated whether AP001885.4 affected c-myc in an m6A-dependent way. Knockdown of AP001885.4 reduced the protein expression of METTL3 (an m6A writer) but did not affect ALKBH5 (an m6A eraser) and ELAVL1 (an m6A reader) (Figure 3D). Knocking down AP001885.4 also diminished the METTL3 mRNA level (Figure 3E). Intriguingly, the silence of AP001885.4 suppressed the m6A modification of c-myc mRNA (Figure 3F and G). METTL3 was highly expressed and positively correlated with c-myc expression level in ESCC tissues (Figure 3H–L).

3.4. Knockdown of AP001885.4 downregulates c-myc via restraining histone lactylation- and NF-κB (p65)-dependent transcription activation

In 2019, histone lactylation was first identified by Zhang *et al*. and was recently reported to regulate tumorigenesis by affecting critical genes such as c-myc, ALKBH5, YTHDF1 (Gu et al. 2024; Pandkar et al. 2023; Wang et al. 2024). Accordingly, we explored whether

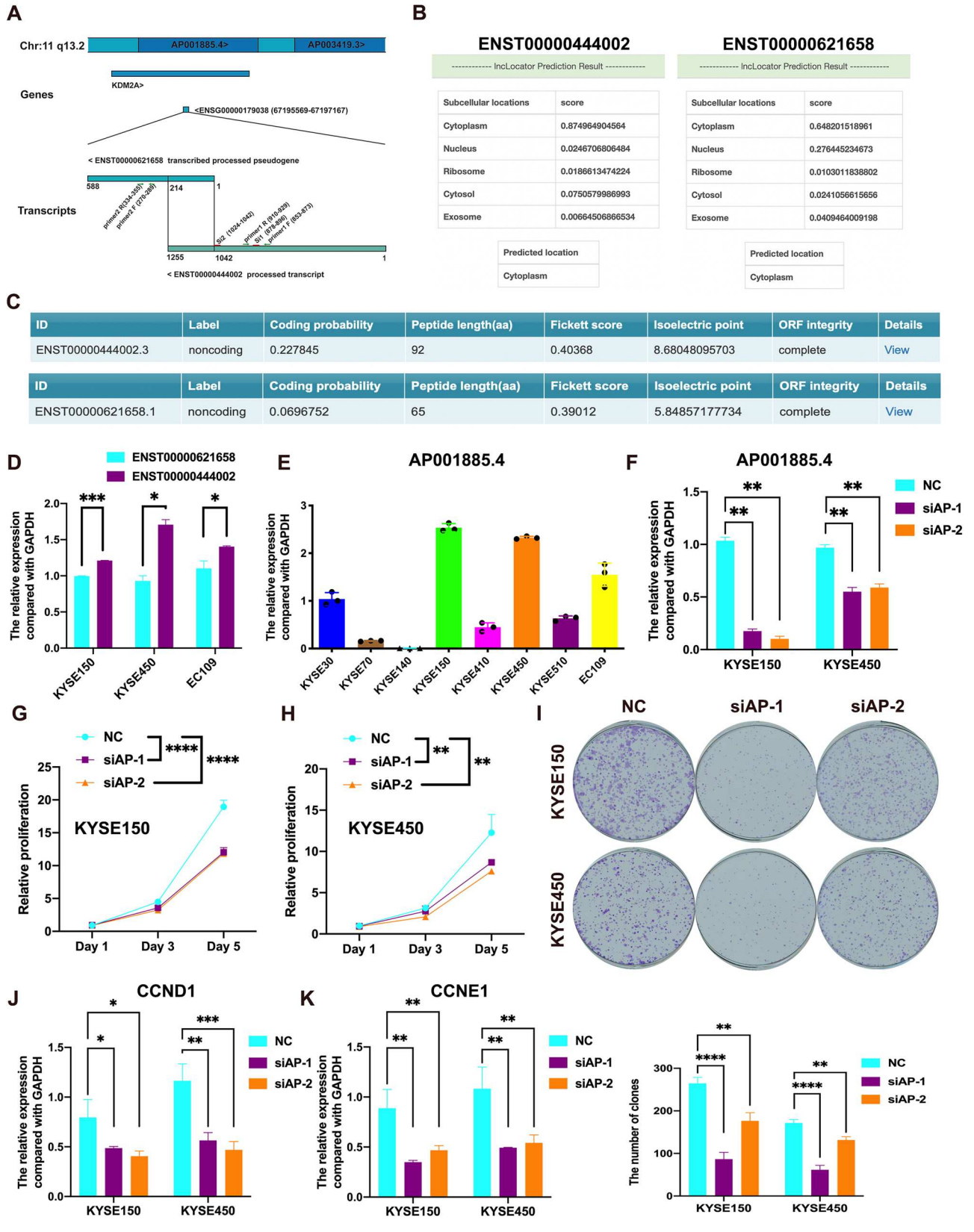

Figure 2. Knockdown of AP001885.4 suppresses the proliferation and colony formation of esophageal squamous cell carcinoma cells. (A) Genomic location of AP001885.4. (B) Sub-cellular location prediction of AP001885.4 using the lncLocator database. (C) Coding potential prediction of AP001885.4 using the CPC2.0 (Coding Potential Calculator 2) database. (D) Expression levels of AP001885.4 two transcripts in KYSE150, KYSE450, and EC109 cells. (E) Expression level of AP001885.4 in 8 ESCC cell lines. (F) Confirmation of knockdown efficiency using qRT-PCR assay. The proliferation of KYSE150 (G) and KYSE450 (H) was detected using CCK-8 assay. (I) Detection of colony formation ability after AP001885.4 knockdown. mRNA levels of CCND1 (J) and CCNE1 (K) were determined by the qRT-PCR method. *, $p < 0.05$; **, $p < 0.01$; ***, $p < 0.001$; ****, $p < 0.0001$.

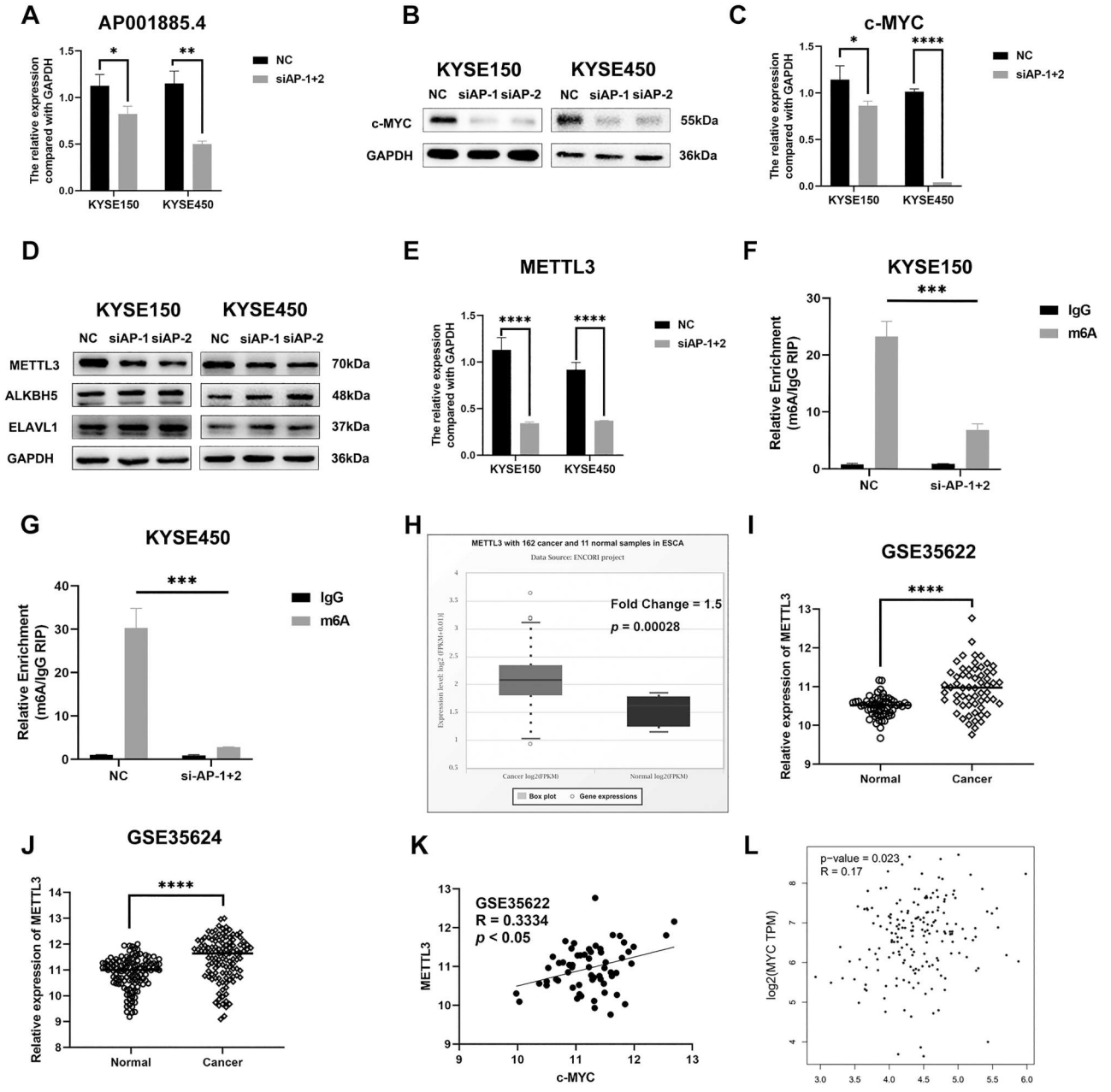

Figure 3. Knockdown of AP001885.4 downregulates c-myc in a METTL3-dependent way. After transfection of AP001885.4 siRNAs, the RNA level of AP001885.4 (A) and protein as well as mRNA levels of c-myc (B and C) were detected using qRT-PCR and Western blot assays. After AP001885.4 knockdown, the protein expression of METTL3, ALKBH5 and ELAVL1 (D) and the mRNA level of METTL3 (E) were measured. The m6A modification of c-myc mRNA was evaluated using RIP assay (F and G). GSE53622 and GSE53624 datasets and TCGA data (in ENCORI and GEPIA databases) were harnessed to analyze METTL3 expression level and correlation between METTL3 and c-myc (H-L). *, $p < 0.05$; **, $p < 0.01$; ***, $p < 0.001$; ****, $p < 0.0001$.

AP001885.4 regulated c-myc by affecting histone lactylation. 50–70% of ATP in tumors was produced by the aerobic glycolysis, therefore, the cellular ATP level could reflect the status of glycolysis, which led to lactate production(Chandel 2021; van Noorden et al. 2024). Intriguingly, knocking down AP001885.4 reduced the levels of ATP, lactate, H3K18 lactylation, and global protein lactylation in ESCC cells (Figure 4A–D). 2-deoxy-D-glucose (2-DG, a non-metabolizable glucose analog) and oxamate (a LDHA inhibitor) are often used to block lactylation in cancer cells (Figure 4E) (Xie et al. 2023). As shown in the Figure 4F and G, 2-DG (8 mM) and oxamate (20 mM) remarkably declined the H3K18 lactylation level. Strikingly, 2-DG and oxamate treatment downregulated c-myc in protein and mRNA levels (Figure 4H–K). Depletion of LDHA and LDHB could suppress lactylation by restraining lactate production. Silence of LDHA also diminished

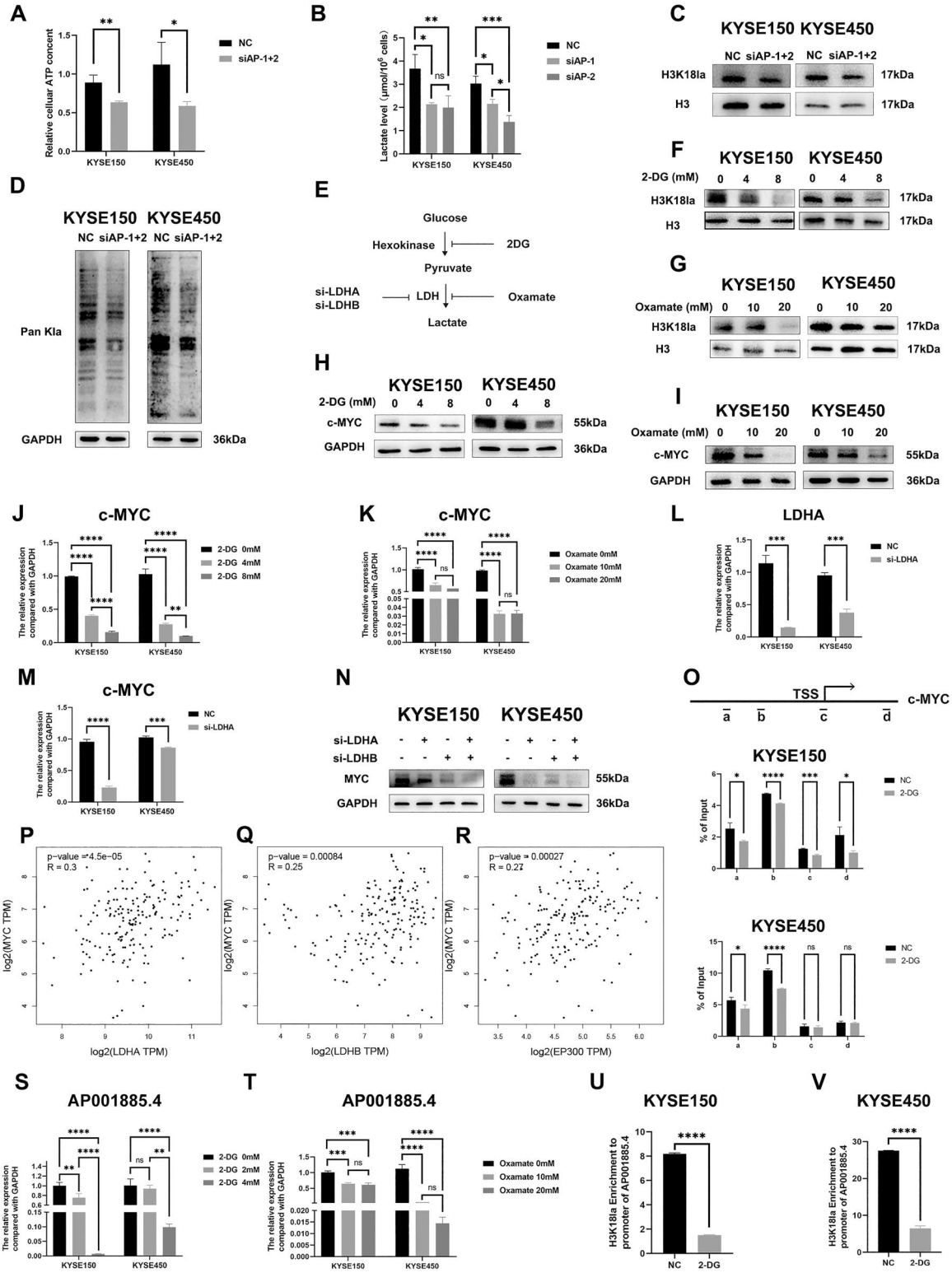

Figure 4. Knockdown of AP001885.4 downregulates c-myc via restraining histone lactylation. After AP001885.4 knockdown, ATP level (A), lactate level (B), H3K18 lactylation level (C), and protein pan-lactylation level (D) were detected using cellular ATP, lactate, and Western blot assays. (E-G) 2-DG and oxamate treatment inhibited H3K18 lactylation and protein pan-lactylation. (H-K) Protein and mRNA levels of c-myc in 2-DG- and oxamate-treated cells were measured using Western blot and qRT-PCR assays. (L-N) mRNA and protein levels of c-myc were detected in LDHA-silenced cells. (O) The histone lactylation in the promoter and coding sequence of *MYC* was detected using ChIP-PCR. (*P*-R) Correlation analysis was performed using TCGA data in the GEPIA database. (S and T) The RNA level of AP001885.4 after 2-DG and oxamate treatment was detected by qRT-PCR technology. (U and V) The H3K18la level in the promoter of AP001885.4 was analyzed using the ChIP-PCR method. ns, no significance; *, $p < 0.05$; **, $p < 0.01$; ***, $p < 0.001$; ****, $p < 0.0001$.

A

Protein ID	RNA ID	Top RNA fragment	Interaction Propensity	Z-score	RBP propensity	Ranking
P00338 LDHA	ENST00000444002.3	901-952	13.61	-0.19	1	0.49192
P07195 LDHB	ENST00000444002.3	901-952	16.4	-0.04	1	0.49846

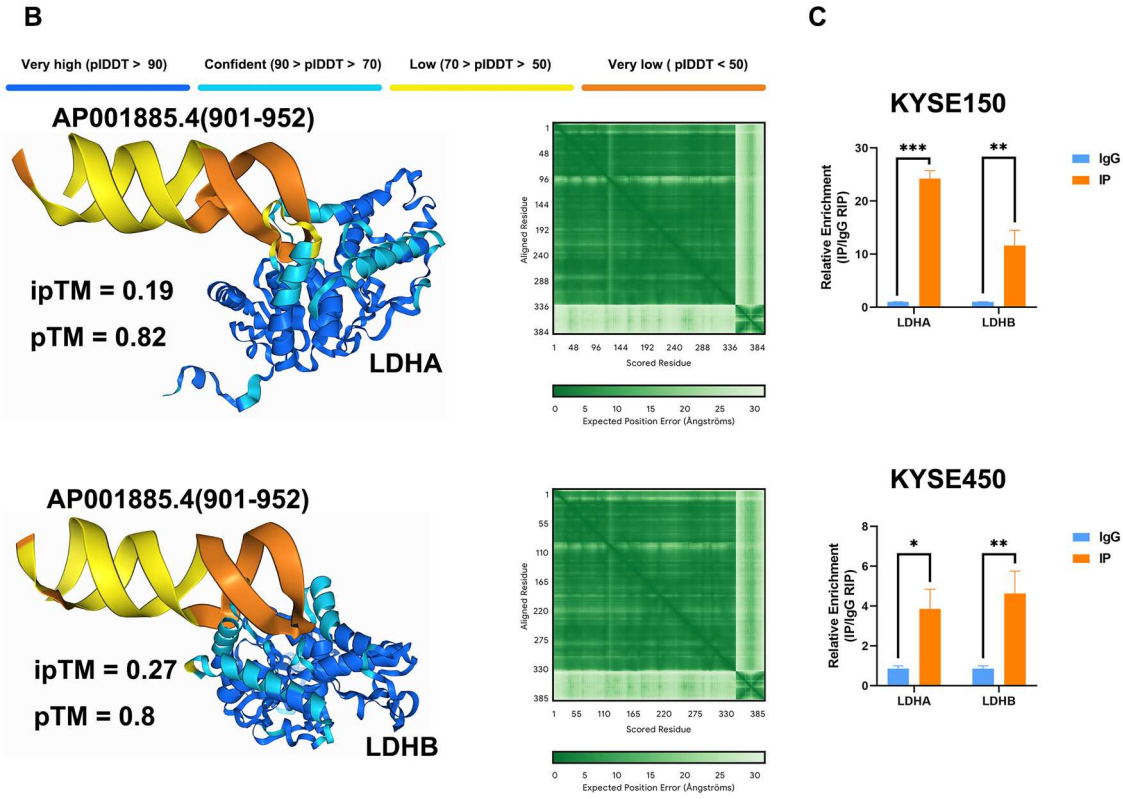

Figure 5. AP001885.4 interacted with LDHA and LDHB in ESCC cells. (A) AP001885.4 interacted proteins including LDHA and LDHB were predicted using the catRAPID software. (B) The complex of AP001885.4 and LDHA/LDHB was analyzed using the AlphaFold 3 software. (C) The interaction of AP001885.4 and LDHA/LDHB was detected using the RIP method. *, $p < 0.05$; **, $p < 0.01$; ***, $p < 0.001$.

c-myc mRNA and protein levels (Figure 4L–N). Histone lactylation at histone H3 lysine K18 (H3K18) could directly activate gene transcription (Zhang et al. 2019). Therefore, we investigated whether 2-DG treatment changed the H3K18 lactylation (H3K18la) level of the *MYC* gene promoter. Results showed that 2-DG reduced the H3K18la level of the *MYC* gene promoter in KYSE150 and KYSE450 cells (Figure 4O). The expression level of c-myc was significantly positively correlated with lactylation-driven genes including LDHA, LDHB, and EP300 in the TCGA-ESCA data (Figure 4P–R). Intriguingly, 2-DG and oxamate treatment also reduced the RNA and H3K18la levels of AP001885.4 in ESCC cells (Figure 4S–V).

LDHA and LDHB were predicted to bind with AP001885.4 by using an application named catRAPID (Figure 5A). Then we confirmed the interaction between AP001885.4 (RNA fragment: 901–952) and LDHA/LDHB using alphafold3 software (Figure 5B). Importantly, the RIP method verified the interaction between LDHA/LDHB and AP001885.4 in KYSE150 and KYSE450 cells (Figure 5C). These data suggest AP001885.4 might regulate lactate-dependent lactylation by binding and affecting LDHA and LDHB.

c-myc is transcriptionally regulated by the NF-κB signaling pathway (Nasrollahzadeh et al. 2020; Wang et al. 2022). Thus, we further investigated whether AP001885.4 regulated c-myc via affecting the NF-κB pathway. Suppression of AP001885.4 downregulated NF-κB (p65) protein and mRNA levels in ESCC cells (Figure 6A and B). Interestingly, JSH-23, an inhibitor of the NF-κB signaling pathway, remarkably diminished

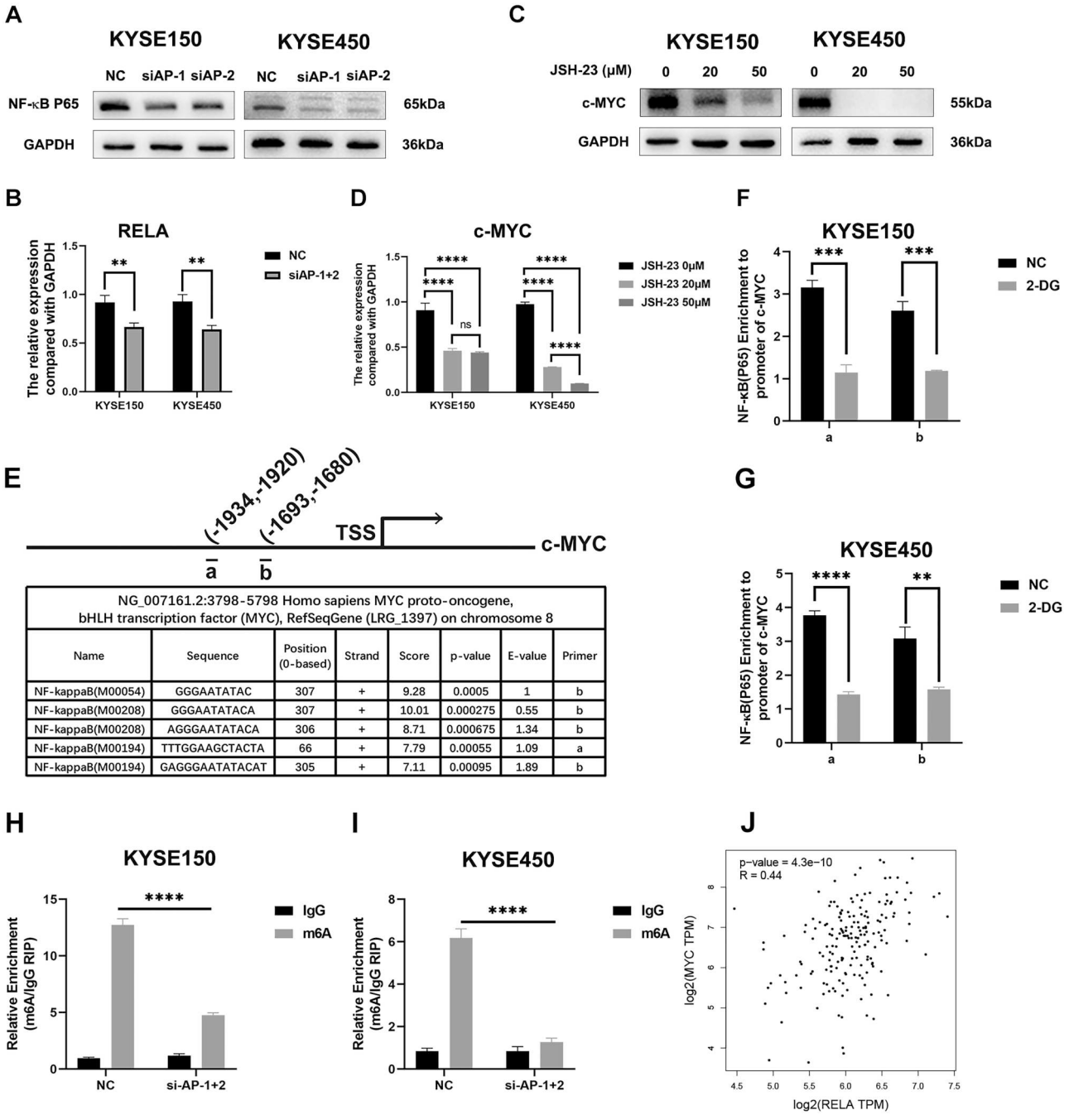

Name	Sequence	Position (0-based)	Strand	Score	p-value	E-value	Primer
NF-kappaB(M00054)	GGGAATATAC	307	+	9.28	0.0005	1	b
NF-kappaB(M00208)	GGGAATATACA	307	+	10.01	0.000275	0.55	b
NF-kappaB(M00208)	AGGGAATATACA	306	+	8.71	0.000675	1.34	b
NF-kappaB(M00194)	TTTGGAAGCTACTA	66	+	7.79	0.00055	1.09	a
NF-kappaB(M00194)	GAGGGAATATACAT	305	+	7.11	0.00095	1.89	b

Figure 6. Knockdown of AP001885.4 downregulates c-myc via inactivating NF-κB signaling pathway. (A) Protein and mRNA levels of NF-κB (p65; gene name: *RELA*) after AP001885.4 knockdown were detected using Western blot and qRT-PCR methods. (C and D) Protein and mRNA levels of c-myc were measured by Western blot and qRT-PCR assays. (E-G) The binding ability between NF-κB (p65) and the promoter of *MYC* was detected using the ChIP-PCR assay. (H and I) The m6A level of NF-κB (p65) was detected using the RIP-PCR method. (J) Correlation between NF-κB (p65) and c-myc was analyzed using the GEPIA database. **, $p < 0.01$; ***, $p < 0.001$; ****, $p < 0.0001$.

the c-myc mRNA and protein expression (Figure 6C and D). The JASPAR database predicted candidate binding sites of NF-κB (p65) in the promoter of the *MYC* gene (Figure 6E), and ChIP-PCR results showed that 2-DG treatment reduced the binding abilities between NF-κB (p65) and the promoter of the *MYC* gene (Figure 6F and G). Intriguingly, the silence of AP001885.4 also reduced the m6A level of NF-κB (p65) mRNA (Figure 6H and I). MYC and NF-κB (p65) were positively correlated at the mRNA level (Figure 6J).

In summary, our results indicated that AP001885.4 was overexpressed in ESCC cells because of a higher

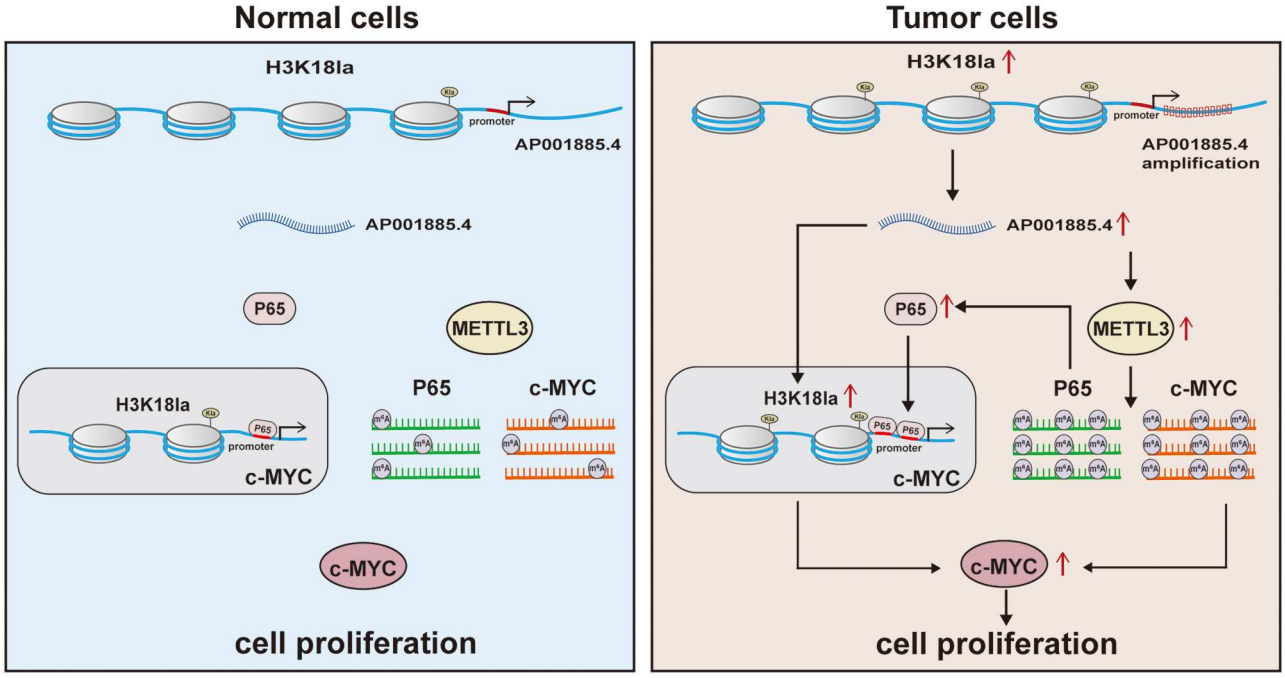

Figure 7. The main findings of this article.

H3K18la level in the promoter and amplification, then enhanced histone lactylation- and NF-κB (p65)-dependent transcription activation and METTL3-mediated mRNA stability of c-myc eventually upregulated c-myc and promoted cell proliferation (Figure 7).

4. Discussion

After analyzing the TCGA data, AP001885.4 was selected as a unique overexpressed and poor prognosis-associated lncRNA in ESCA. AP001885.4 is located in the intron of the *KDM2A* gene (11q13.2), which chromosome region is gained in 69.6% of ESCC cases (Shi et al. 2013). Therefore, amplification contributes to AP001885.4 overexpression.

Our results demonstrated that in ESCC cells, AP001885.4 positively regulated c-myc. c-myc was previously reported to be overexpressed in ESCC, and its overexpression was associated with a shorter survival time of patients(Ma et al. 2022; Roohinejad et al. 2023). Mechanically, c-myc was regulated by CCT6A (Xia et al. 2023), HCP5-UTP3 axis (Nan et al. 2023), β-catenin (Ma et al. 2022) in ESCC. Some studies focused on the regulatory connection between lncRNA and c-myc in ESCC. LINC00858 could improve myc expression via regulating ZNF184-FTO axis (Ke et al. 2023). Interaction of SLC25A21-AS1 and NPM1 could promote the transcriptional activity of c-myc (Liu et al. 2022). SNHG17 was overexpressed in ESCC and enhanced c-myc transcription via recruiting c-Jun to the promoter of c-myc (Shen et al. 2022). Our results further indicated that AP001885.4 was also a critical upstream regulator of c-myc in ESCC.

Our study proved that, in ESCC, AP001885.4 upregulated c-myc through increasing METTL3. METTL3 expression was positively correlated with poor prognosis of ESCC patients, and METTL3 improved the proliferation of ESCC cells via regulating IFIT2 in an m6A-dependent manner (Ge et al. 2022; Zhou et al. 2022). Another study reported that silencing METTL3 could reduce the m6A modification level of AMIGO2 5'UTR, and suppressed AMIGO2 expression and ESCC cell proliferation (Qiu et al. 2024). Strikingly, our results suggested that the AP001885.4-METTL3 axis was also the upstream regulator of c-myc in ESCC.

Significantly, our data further demonstrated that AP001885.4 positively regulated c-myc via histone lactylation and NF-κB-dependent manner. Up to now, the role of lactylation of histone and non-histone proteins in ESCC is unknown. Our study found that knockdown of AP001885.4 suppressed H3K18 lactylation and protein pan-lactylation, and blocking lactylation using 2-DG and oxamate diminished c-myc expression, indicating AP110885.4 upregulated c-myc via a histone lactylation-dependent manner. Histone lactylation could transcriptionally activate gene expression. Histone lactylation boosted LINC01127 expression in glioblastoma stem cells and promoted PD-L1 transcription in acute myeloid leukemia (Huang et al. 2023; Li et al. 2023). After analyzing the interacted proteins of AP001885.4

using catRAPID and Alphafold3 softwares and validating using the RIP method, the lactylation-driven genes LDHA and LDHB were found to be interacted with AP001885.4, indicating AP001885.4 might participate in the lactylation process via biding and regulating LDHA and LDHB. Importantly, our data also found that blocking lactylation using 2-DG and oxamate reduced AP001885.4 expression, indicative of histone lactylation contributed to AP001885.4 overexpression. c-myc is a target gene of the NF-κB signaling pathway (Nasrollahzadeh et al. 2020; Wang et al. 2022), and our results further confirmed that knockdown of AP001885.4 downregulated NF-κB (p65) and JSH-23, an inhibitor of NF-κB signaling pathway, reduced c-myc expression, indicative of AP110885.4 upregulated c-myc dependent on NF-κB.

Albeit we unveiled that AP001885.4 enhanced the colony formation and proliferation of ESCC cells via augmenting c-myc, there are still some limitations in our study. Whether overexpressing AP001885.4 could promote the proliferation and colony formation of ESCC cells, and the mechanisms underlying how AP001885.4 regulated NF-κB and how AP001885.4 regulated METTL3 are still unclear.

5. Conclusion

Our results indicated that AP001885.4 promoted the proliferation of esophageal squamous cell carcinoma cells by histone lactylation- and NF-κB (p65)-dependent transcription activation and METTL3-mediated mRNA stability of c-myc.

Availability of data and materials

The data used to support the findings of this study are available from the corresponding author upon request.

Declaration of interest statement

The authors report no declarations of interest.

Disclosure statement

No potential conflict of interest was reported by the author(s).

Funding

This study was funded by the National Natural Science Foundation of China [grant number 82160585] and Joint Medical Program of Kunming University of Science and Technology [grant number KUST-KH2022001Z, KUST-PE2022002Z and KUST-KH2023016Y] and the innovation team of oxidative stress and defense of Yunnan Province [grant number 202305AS350011] and Chest Disease Clinical Medical Center of The First People's Hospital of Yunnan Province [grant number 2022LCZXKF-XB01].

Ethical approval

The Medical Ethics Committee of Kunming University of Science and Technology approved this study.

References

Arnold M, Soerjomataram I, Ferlay J, Forman D. 2015. Global incidence of oesophageal cancer by histological subtype in 2012. Gut. 64:381–387. doi:10.1136/gutjnl-2014-308124.

Bellucci M, Agostini F, Masin M, Tartaglia GG. 2011. Predicting protein associations with long noncoding RNAs. Nat Methods. 8:444–445. doi:10.1038/nmeth.1611.

Cancer Genome Atlas N. 2015. Comprehensive genomic characterization of head and neck squamous cell carcinomas. Nature. 517:576–582. doi:10.1038/nature14129.

Chandel NS. 2021. Glycolysis. Cold Spring Harb Perspect Biol. 13:a040535.

Chen J, Duan Z, Liu Y, Fu R, Zhu C. 2022. Ginsenoside Rh4 suppresses metastasis of esophageal cancer and expression of c-Myc via targeting the Wnt/beta-catenin signaling pathway. Nutrients. 14:3042. doi:10.3390/nu14153042

Chen K, Wang X, Wei B, Sun R, Wu C, Yang HJ. 2022. LncRNA SNHG6 promotes glycolysis reprogramming in hepatocellular carcinoma by stabilizing the BOP1 protein. Anim Cells Syst (Seoul). 26:369–379. doi:10.1080/19768354.2022.2134206

Cui Y, Yan M, Wu W, Lv P, Wang J, Huo Y, Lou Y, Ma X, Chang J, Guan F, et al. 2022. ESCCAL-1 promotes cell-cycle progression by interacting with and stabilizing galectin-1 in esophageal squamous cell carcinoma. NPJ Precis Oncol. 6:12. doi:10.1038/s41698-022-00255-x.

Ge F, Li Z, Hu J, Pu Y, Zhao F, Kong L. 2022. METTL3/m(6)A/IFIT2 regulates proliferation, invasion and immunity in esophageal squamous cell carcinoma. Front Pharmacol. 13:1002565. doi:10.3389/fphar.2022.1002565.

Gu X, Zhuang A, Yu J, Yang L, Ge S, Ruan J, Jia R, Fan X, Chai P. 2024. Histone lactylation-boosted ALKBH3 potentiates tumor progression and diminished promyelocytic leukemia protein nuclear condensates by m1A demethylation of SP100A. Nucleic Acids Res. 52:2273–2289. doi:10.1093/nar/gkad1193

Hu X, Moon JW, Li S, Xu W, Wang X, Liu Y, Lee JY. 2016. Amplification and overexpression of CTTN and CCND1 at chromosome 11q13 in esophagus squamous cell carcinoma (ESCC) of North Eastern Chinese Population. Int J Med Sci. 13:868–874. doi:10.7150/ijms.16845.

Huang ZW, Zhang XN, Zhang L, Liu LL, Zhang JW, Sun YX, Xu JQ, Liu Q, Long ZJ. 2023. STAT5 promotes PD-L1 expression by facilitating histone lactylation to drive immunosuppression in acute myeloid leukemia. Signal Transduct Target Ther. 8(1):391. doi:10.1038/s41392-023-01605-2.

Ke S, Wang J, Lu J, Fang M, Li R. 2023. Long intergenic non-protein coding RNA 00858 participates in the occurrence and development of esophageal squamous cell carcinoma through the activation of the FTO-m6A-MYC axis by recruiting ZNF184. Genomics. 115:110593. doi:10.1016/j.ygeno.2023.110593.

Lee HY, Cha J, Kim SK, Park JH, Song KH, Kim P, Kim MY. 2019. . c-MYC drives breast cancer metastasis to the brain, but promotes synthetic lethality with TRAIL. Mol Cancer Res. 17:544–554. doi:10.1158/1541-7786.MCR-18-0630.

Li L, Li Z, Meng X, Wang X, Song D, Liu Y, Xu T, Qin J, Sun N, Tian K, et al. 2023. Histone lactylation-derived LINC01127 promotes the self-renewal of glioblastoma stem cells via the cis-regulating the MAP4K4 to activate JNK pathway. Cancer Lett. 579:216467. doi:10.1016/j.canlet.2023.216467.

Li Q, Zhang Z, Jiang H, Hou J, Chai Y, Nan H, Li F, Wang L. 2022. DLEU1 promotes cell survival by preventing DYNLL1 degradation in esophageal squamous cell carcinoma. J Transl Med. 20:245. doi:10.1186/s12967-022-03449-w.

Liu Y, Li C, Fang L, Wang L, Liu H, Tian H, Zheng Y, Fan T, He J. 2022. Lipid metabolism-related lncRNA SLC25A21-AS1 promotes the progression of oesophageal squamous cell carcinoma by regulating the NPM1/c-Myc axis and SLC25A21 expression. Clin Transl Med. 12:e944. doi:10.1002/ctm2.944.

Luo XJ, He MM, Liu J, Zheng JB, Wu QN, Chen YX, Meng Q, Luo KJ, Chen DL, Xu RH, et al. 2022. LncRNA TMPO-AS1 promotes esophageal squamous cell carcinoma progression by forming biomolecular condensates with FUS and p300 to regulate TMPO transcription. Exp Mol Med. 54:834–847. doi:10.1038/s12276-022-00791-3.

Ma ZQ, Feng YT, Guo K, Liu D, Shao CJ, Pan MH, Zhang YM, Zhang YX, Lu D, Huang D, et al. 2022. Melatonin inhibits ESCC tumor growth by mitigating the HDAC7/beta-catenin/c-Myc positive feedback loop and suppressing the USP10-maintained HDAC7 protein stability. Mil Med Res. 27(9):54.

Mei LL, Wang WJ, Qiu YT, Xie XF, Bai J, Shi ZZ. 2017. miR-145-5p suppresses tumor cell migration, invasion and epithelial to mesenchymal transition by regulating the Sp1/NF-κB signaling pathway in esophageal squamous cell carcinoma. Int J Mol Sci. 18:1833. doi:10.3390/ijms18091833

Meskyte EM, Keskas S, Ciribilli Y. 2020. MYC as a multifaceted regulator of tumor microenvironment leading to metastasis. Int J Mol Sci. 21:7710. doi:10.3390/ijms21207710

Nair L, Chung H, Basu U. 2020. Regulation of long non-coding RNAs and genome dynamics by the RNA surveillance machinery. Nat Rev Mol Cell Biol. 21:123–136. doi:10.1038/s41580-019-0209-0.

Nan Y, Luo Q, Wu X, Chang W, Zhao P, Liu S, Liu Z. 2023. HCP5 prevents ubiquitination-mediated UTP3 degradation to inhibit apoptosis by activating c-Myc transcriptional activity. Mol Ther. 31:552–568. doi:10.1016/j.ymthe.2022.10.006.

Nasrollahzadeh A, Bashash D, Kabuli M, Zandi Z, Kashani B, Zaghal A, Mousavi SA, Ghaffari SH. 2020. Arsenic trioxide and BIBR1532 synergistically inhibit breast cancer cell proliferation through attenuation of NF-κB signaling pathway. Life Sci 257:118060. doi:10.1016/j.lfs.2020.118060.

Ohashi S, Miyamoto S, Kikuchi O, Goto T, Amanuma Y, Muto M. 2015. Recent advances from basic and clinical studies of esophageal squamous cell carcinoma. Gastroenterology. 149:1700–1715. doi:10.1053/j.gastro.2015.08.054.

Pandkar MR, Sinha S, Samaiya A, Shukla S. 2023. Oncometabolite lactate enhances breast cancer progression by orchestrating histone lactylation-dependent c-Myc expression. Transl Oncol. 37:101758. doi:10.1016/j.tranon.2023.101758.

Qiu Y, Tian Z, Miao TY, Shen L, Chen J, Li PF, Zhu ZX, Zhu ZF, Wu WJ, Xu X, et al. 2024. The METTL3-m(6)A-YTHDC1-AMIGO2 axis contributes to cell proliferation and migration in esophageal squamous cell carcinoma. Gene. 908:148281. doi:10.1016/j.gene.2024.148281.

Ren L, Fang X, Shrestha SM, Ji Q, Ye H, Liang Y, Liu Y, Feng Y, Dong J, Shi R. 2022. LncRNA SNHG16 promotes development of oesophageal squamous cell carcinoma by interacting with EIF4A3 and modulating RhoU mRNA stability. Cell Mol Biol Lett. 27:89. doi:10.1186/s11658-022-00386-w.

Roh J, Im M, Kang J, Youn B, Kim W. 2023. Long non-coding RNA in glioma: novel genetic players in temozolomide resistance. Anim Cells Syst (Seoul). 27:19–28. doi:10.1080/19768354.2023.2175497.

Roohinejad Z, Bahramian S, Shamsabadi FT, Sahebi R, Amini A, Sabour D, Shafiee M. 2023. Upregulation of the c-MYC oncogene and adjacent long noncoding RNAs PVT1 and CCAT1 in esophageal squamous cell carcinoma. BMC Cancer. 23:34. doi:10.1186/s12885-022-10464-z.

Shen S, Liang J, Liang X, Wang G, Feng B, Guo W, Guo Y, Dong Z. 2022. SNHG17, as an EMT-related lncRNA, promotes the expression of c-Myc by binding to c-Jun in esophageal squamous cell carcinoma. Cancer Sci 113:319–333. doi:10.1111/cas.15184.

Shi ZZ, Liang JW, Zhan T, Wang BS, Lin DC, Liu SG, Hao JJ, Yang H, Zhang Y, Zhan QM, et al. 2011. Genomic alterations with impact on survival in esophageal squamous cell carcinoma identified by array comparative genomic hybridization. Genes Chromosomes Cancer. 50:518–526. doi:10.1002/gcc.20875.

Shi ZZ, Shang L, Jiang YY, Hao JJ, Zhang Y, Zhang TT, Lin DC, Liu SG, Wang BS, Gong T, et al. 2013. Consistent and differential genetic aberrations between esophageal dysplasia and squamous cell carcinoma detected by array comparative genomic hybridization. Clin Cancer Res. 19:5867–5878. doi:10.1158/1078-0432.CCR-12-3753.

Shi ZZ, Wang WJ, Chen YX, Fan ZW, Xie XF, Yang LY, Chang C, Cai Y, Hao JJ, Wang MR, et al. 2020. The miR-1224-5p/TNS4/EGFR axis inhibits tumour progression in oesophageal squamous cell carcinoma. Cell Death Dis 11:597. doi:10.1038/s41419-020-02801-6.

Smyth EC, Gambardella V, Cervantes A, Fleitas T. 2021. Checkpoint inhibitors for gastroesophageal cancers: dissecting heterogeneity to better understand their role in first-line and adjuvant therapy. Ann Oncol. 32:590–599. doi:10.1016/j.annonc.2021.02.004.

van Noorden CJF, Yetkin-Arik B, Serrano Martinez P, Bakker N, van Breest Smallenburg ME, Schlingemann RO, Klaassen I, Majc B, Habic A, Bogataj U, et al. 2024. New insights in ATP synthesis as therapeutic target in cancer and angiogenic ocular diseases. J Histochem Cytochem. 72:329–352. doi:10.1369/00221554241249515

Wang J, Liu X, Li P, Wang J, Shu Y, Zhong X, Gao Z, Yang J, Jiang Y, Zhou X, et al. 2022. Long noncoding RNA HOTAIR regulates the stemness of breast cancer cells via activation of the NF-kappaB signaling pathway. J Biol Chem. 298:102630. doi:10.1016/j.jbc.2022.102630.

Wang P, Xie D, Xiao T, Cheng C, Wang D, Sun J, Wu M, Yang Y, Zhang A, Liu Q. 2024. H3k18 lactylation promotes the progression of arsenite-related idiopathic pulmonary fibrosis via YTHDF1/m6A/NREP. J Hazard Mater. 461:132582. doi:10.1016/j.jhazmat.2023.132582.

Xia X, Zhao S, Chen W, Xu C, Zhao D. 2023. CCT6A promotes esophageal squamous cell carcinoma cell proliferation,

invasion and epithelial-mesenchymal transition by activating TGF-beta/Smad/c-Myc pathway. Ir J Med Sci. 192:2653–2660. doi:10.1007/s11845-023-03357-y

Xie B, Lin J, Chen X, Zhou X, Zhang Y, Fan M, Xiang J, He N, Hu Z, Wang F. 2023. CircXRN2 suppresses tumor progression driven by histone lactylation through activating the Hippo pathway in human bladder cancer. Mol Cancer. 22:151. doi:10.1186/s12943-023-01856-1

Zhang D, Tang Z, Huang H, Zhou G, Cui C, Weng Y, Liu W, Kim S, Lee S, Perez-Neut M, et al. 2019. Metabolic regulation of gene expression by histone lactylation. Nature. 574:575–580. doi:10.1038/s41586-019-1678-1.

Zheng RS, Zhang SW, Sun KX, Chen R, Wang SM, Li L, Zeng HM, Wei WW, He J. 2023. Cancer statistics in China, 2016. Zhonghua Zhong Liu Za Zhi. 45:212–220.

Zhou Y, Guo S, Li Y, Chen F, Wu Y, Xiao Y, An J. 2022. METTL3 is associated With the malignancy of esophageal squamous cell carcinoma and serves as a potential immunotherapy biomarker. Front Oncol. 12:824190. doi:10.3389/fonc.2022.824190.